

Coherence attribute applications on seismic data in various guises

Satinder Chopra*[†] and Kurt J. Marfurt⁺

[†]Arcis Seismic Solutions, TGS, Calgary; ⁺The University of Oklahoma, Norman

Summary

The iconic coherence attribute is very useful for geologic feature imaging such as faults, deltas, submarine canyons, karst collapse, mass transport complexes, and more. Besides its preconditioning, the interpretation of discrete stratigraphic features on seismic data is also limited by its bandwidth, where in general the data with higher bandwidth yields crisper features than data with lower bandwidth. Some form of spectral balancing applied to the seismic amplitude data can help in achieving such an objective, so that coherence run on spectrally balanced seismic data yields a better definition of the geologic features of interest. The quality of the generated coherence attribute is also dependent in part on the algorithm employed for its computation. In the eigenstructure decomposition procedure for coherence computation, spectral balancing equalizes each contribution to the covariance matrix, and thus yields crisper features on coherence displays. There are other ways to *modify the spectrum of the input data* in addition to simple spectral balancing, including the amplitude-volume technique, taking the derivative of the input amplitude, spectral bluing, and thin-bed spectral inversion. We compare some of those techniques, and show their added value in seismic interpretation.

Introduction

Since its introduction at the 1992 SEG Annual Meeting, the coherence attribute has come a long way. As an iconic attribute, it finds its place in most workstation interpretation software packages, and for good reason. Because three-dimensionality is an essential ingredient of the coherence volume computation, geologic features that are not easily seen on a single slice become much more apparent, with faults, deltas, submarine canyons, karst collapse, mass transport complexes, and many other geologic features appearing clearly on coherence displays.

The interpretation of discrete stratigraphic features on seismic data is limited by its bandwidth. Seismic data that have a higher bandwidth yield crisper and more detailed images than the same data with lower bandwidth. Some form of spectral balancing on the seismic data prior to attribute computation helps in achieving such an objective. If the underlying reflectivity can be considered to be random, after spectral balancing, the spectral contribution of the seismic wavelet are largely removed, allowing the analysis of tuned reflections that occur at layers exhibiting quarter wavelength thickness. Quantitative measurement of such tuning is achieved through different spectral decomposition methods (e.g. Partyka et al., 1999; Marfurt and Kirilin, 2001) where one computes a suite of spectral magnitude and phase components

obtained from the original broadband seismic data. Less commonly used by interpreters, the spectral voice components often provide additional insight into the subsurface features (Chopra and Marfurt, 2016). Going one step further, coherence computed from such spectral voice components can highlight discontinuities that are preferentially imaged by a given spectral component.

Vernengo and Trincherro (2015) described the application of amplitude-volume-technique (AVT) workflow that aids seismic interpretation. It entails the calculation of the root-mean-square (RMS) of the seismic amplitudes in a definite analysis window and then rotate the phase of the data by -90° , by using the mathematical operation of Hilbert transform. Such a calculation of the input seismic data yields somewhat higher amplitudes of the frequencies in the bandwidth of the data. We demonstrate the application of the coherence attribute on input seismic data, on the same data after spectral balancing, as well as spectral magnitude and voice components obtained after carrying out spectral decomposition using continuous wavelet transform approach. Finally, we also include the application of coherence attribute on seismic data passed through the AVT workflow, and compare the results. Finally, we combine the coherence computed on different voice components into a single composite image, a process referred to as multispectral coherence (Marfurt, 2017).

Alternative coherence algorithms

The different coherence algorithms that have been proposed over time are the crosscorrelation-based (Bahorich and Farmer, 1995), semblance-based (Marfurt et al., 1998), variance-based coherence (Pepper and Bejarano, 2005), eigenstructure-based (Gersztenkorn and Marfurt, 1999), prediction error filter-based (Bednar, 1998) and gradient structure tensor-based (Bakker, 2003). These algorithms vary in how they handle seismic character variability and thus have different sensitivities to geology, spectral bandwidth and seismic noise. Out of these the most common algorithms available in workstation software packages are the semblance and some form of eigenstructure decomposition. Here we restrict our analysis to application of energy-ratio coherence, which is based on a variation of the eigenstructure approach.

Integration of coherence and spectral decomposition

Spectral decomposition

The process of spectral decomposition decomposes the seismic data into individual frequency components that fall within the

measured seismic bandwidth, so that subsurface geology can be seen at different frequencies. This process aids the interpretation of discrete stratigraphic features that are limited by both the bandwidth and signal-to-noise ratio of the input seismic data. Tuned seismic reflections that show the maximum amplitudes at quarter wavelength can be examined at higher frequencies for better delineation of target zones. Similarly, while through-going faults may be seen at both low and high frequency components, more localized smaller faults may only be seen at the higher frequency components.

Spectral decomposition is carried out by transforming the seismic data from the time domain into the frequency domain. This can be done simply by using the discrete Fourier transform (Partyka et al., 1999; Marfurt and Kirlin, 2001) with a fixed length short window. There are other methods that could be used for the purpose, such as the continuous wavelet transform (Sinha et al., 2005), the S-transform (Stockwell, 1996), or the matching pursuit decomposition (Mallat and Zhang, 1993; Castagna et al., 2003). Each of these methods have their own applicability and limitations, and the choice of a particular method could also depend on the end objective. The continuous wavelet transform depends on the choice of the mother wavelet, and usually yields higher spectral resolution but reduced temporal resolution. Using any of the above spectral decomposition methods, the input seismic data volume can be decomposed into amplitude and phase volumes at discrete frequencies within the bandwidth of the data.

The mother wavelet chosen for CWT spectral decomposition, e.g. the Morlet wavelet, is a complex function (Sinha et al. 2003), and so the spectral components obtained from CWT are also complex. Thus, when spectral decomposition is carried out on seismic data, it yields the spectral magnitude and phase at each time-frequency sample. The spectral magnitude represents the square-root of the energy that correlates with the trace, while the spectral phase represents the phase rotation between the seismic trace and the Morlet wavelet at each instant of time.

Voice components

In addition to the spectral and phase components, Goupillaud et al. (1984) introduced another component, called the voice component, which is a simple function of spectral magnitude, a_m , and phase ϕ_m , at each time-frequency sample for trace m and is given by

$$a_m(t, f) = a_m(t, f)\exp[-i\phi_m(t, f)]. \quad (1)$$

The real part of the sum over all frequencies, f , of all these voice components reconstructs the original trace. Since the voice components are band-pass filtered versions of the original seismic data (Fahmy et al., 2008) application to map subtle hydrocarbon features can be viewed as analysis of the spectral voices.

After choosing an appropriate mother wavelet (Chopra and Marfurt, 2015) the scaled members of the wavelet family are defined by simple scaling and shifting of the mother wavelet. Crosscorrelating the member wavelets with the original seismic trace generates the spectral voice components. For the continuous wavelet transform, the voice components are equivalent to narrow bandpass filtered versions of the input seismic data.

When the energy-ratio coherence is run on the individual voice components, the time or horizon slices from the coherence volume indicate the lineaments in significantly more clarity and definition (Chopra and Marfurt, 2016). Three coherence displays that exhibit the lineament definitions better than the others can be blended with three colors (red, green and blue) so as to integrate the information in individual datasets for ease in comparison, viewing and hence its interpretation (Li and Lu, 2014 and Honorio et al., 2017). Careful examination of the blended images quantitatively confirms that different frequencies are more or less sensitive to a different fault. While effective, the limitation of this color display tool is that one is limited to showing only three components at a given time.

Sui et al. (2015) addressed the multispectral coherence analysis problem by constructing a covariance matrix from the spectral magnitudes a_m :

$$C_{mn} = \sum_{l=1}^L \sum_{k=-K}^K [a(f_l, t_k, x_m, y_m)a(f_l, t_k, x_n, y_n)], \quad (2)$$

where L is the number of spectral components. They found the resulting coherence images to be higher quality than that computed from the broadband data, including most of the details seen in coherence computed by constructing covariance matrices from the individual magnitude components. By ignoring the phase component, they also found that the algorithm was less sensitive to structural dip, resulting in algorithmic simplification.

Marfurt (2017) built on these ideas, but constructed a multispectral covariance matrix oriented along structural dip using the analytic trace, and therefore twice as many sample vectors (i.e. spectral voices and their Hilbert transforms)

$$C_{mn} = \sum_{l=1}^L \sum_{k=-K}^K [u(t_k, f_l, x_m, y_m)u(t_k, f_l, x_n, y_n) + u^H(t_k, f_l, x_m, y_m)u^H(t_k, f_l, x_n, y_n)]. \quad (3)$$

The corresponding energy ratio coherence computed using this equation is then referred to as *multispectral coherence*. We demonstrate the application of this approach on a 3D seismic data from northeast British Columbia, Canada in the following section.

Spectral balancing of input seismic data

Chopra et al., (2011) demonstrated that if the input seismic data are spectrally balanced, or if its frequency bandwidth is extended somehow, the resulting volumes could lead to higher discontinuity detail. Thin-bed spectral inversion (Chopra et al.,

2006; Chopra et al., 2009) is a process that removes the time-variant wavelet from the seismic data and extracts the reflectivity to image thicknesses below seismic resolution using a matching-pursuit variant of sparse-spike inversion. In addition to an enhanced image of thin reservoirs, the frequency-enhanced images have proven useful in mapping subtle onlaps and offlaps, thereby facilitating the mapping of parasequences and the direction of sediment transport. Besides viewing the spectrally broadened seismic data in the form of reflectivity, it can be filtered back to any desired bandwidth that filter panel tests indicate, adding useful information for interpretational purposes. Coherence attribute computation performed on spectrally balanced data yield higher detail about faults and fractures.

Amplitude volume technique attributes

Vernengo and Trincherro (2015) described the application of amplitude volume technique (AVT) to seismic data for enhancing and focusing the subsurface geologic elements, in terms of faults, unconformities, channel edges and thus helping with their interpretation. The AVT attributes was first proposed by Bulhões (1999) and elaborated upon by way of application by Bulhões and de Amorin (2005). The AVT attribute is obtained by calculating the RMS amplitude from the seismic amplitudes in a sliding window down the trace (i.e. calculating the square root of the average of the sum of the squares of the amplitudes). This step is followed by rotating the phase of the data by -90° , through the application of Hilbert transform. The RMS computation (squaring, averaging and taking square root) makes all the amplitudes positive, but the nonlinearity introduced therein modifies the frequency spectrum, enhancing it at the higher end. The -90° phase rotation exercised next changes all the amplitudes into positive and negative values. In Figure 1 we show a segment of a section from the input seismic data and its equivalent AVT section. Notice the higher frequency content and the pseudorelief introduced in the process, which makes the interpretability of the AVT data much better.

We generate energy ratio coherence on two different versions of the input seismic data that we generated and have discussed above. A comparison is made in terms of times slices at 1380 ms shown in Figure 2. We show coherence on input data, when it is spectrally balanced, and compare it with coherence on the same data with AVT. We notice that the coherence on data with spectral balancing enhances the discontinuity detail in the data by way of their crisp definitions, and application of AVT shows all discontinuities much better focused. Application of multispectral coherence on this data exhibits a cleaner look of the coherence displays in Figure 2, and coherence on data after spectral balancing and AVT shows superior definition of discontinuities, especially the east to west lineaments, which would help with their interpretation.

Conclusions

We run energy ratio coherence on input seismic data, and a number of other versions that we generate in terms of voice components obtained by using continuous wavelet transform method of spectral decomposition, spectral balanced version obtained by using thin-bed reflectivity inversion, and AVT attributes. Our comparison of the equivalent time slice displays from the coherence volumes allows us to infer, (a) coherence on spectrally balanced input seismic data yields better lineament detail, (b) coherence on voice components highlights the discontinuities at different frequencies that show better definition, which can be helpful for their interpretation, (c) multispectral coherence displays show crisper definition of lineaments and so are useful, (d) coherence run on the versions of the data discussed above after AVT shows superior definition of lineaments and hence we recommend should be used in their interpretation.

Acknowledgements

We wish to thank Arcis Seismic Solutions/TGS for encouraging this work and also for the permission to present and publish it.

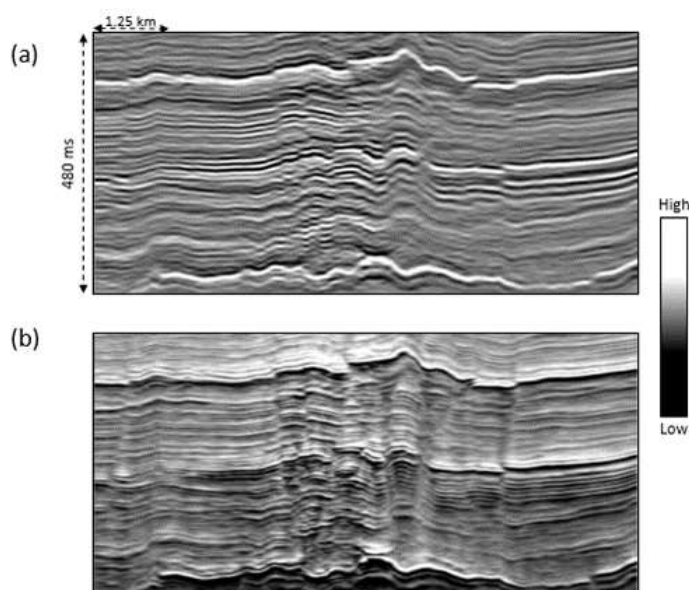


Figure 1: Segment of a (a) seismic section from the input data, and (b) from input data with AVT run on it. The AVT display seems to provide a better guiding interpretation perspective. We use this characteristic for generating coherence on AVT-run data and compare it with data without AVT. Examples from that comparison are shown in Figure 2. (Data courtesy: Arcis Seismic Solutions, TGS, Calgary)

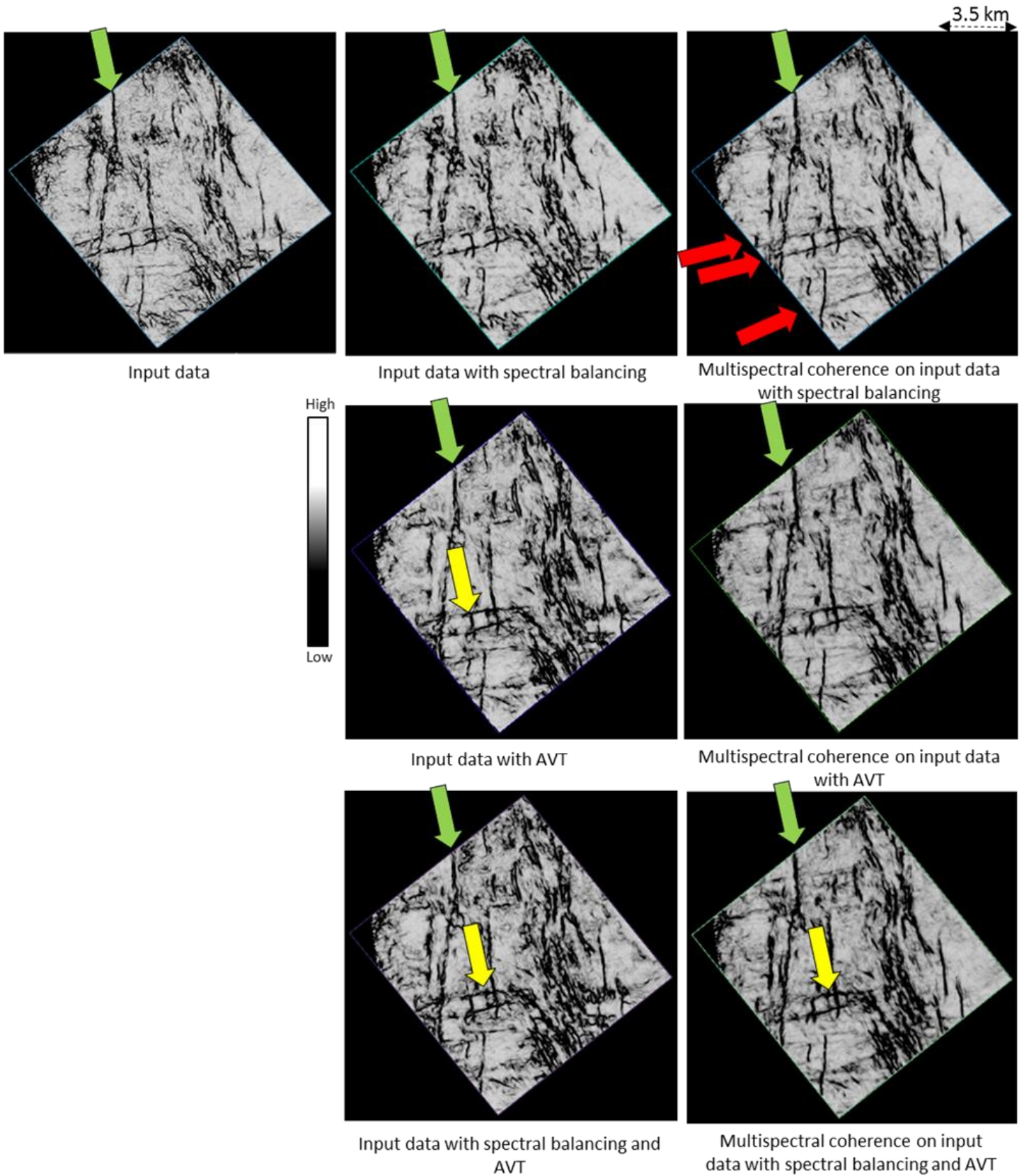


Figure 2: Time slices at $t=1380$ ms through a suite of seven coherence volumes. The volumes with AVT better delineate the fault block indicated by the yellow arrow. AVT and multispectral coherence provide a more continuous fault indicated by the green arrow. Multispectral coherence shows more continuous EW faults indicated by the red arrows. (Data courtesy: Arcis Seismic Solutions, TGS, Calgary)

EDITED REFERENCES

Note: This reference list is a copyedited version of the reference list submitted by the author. Reference lists for the 2017 SEG Technical Program Expanded Abstracts have been copyedited so that references provided with the online metadata for each paper will achieve a high degree of linking to cited sources that appear on the Web.

REFERENCES

- Bahorich, M. S., and S. L. Farmer, 1995, 3-D seismic coherency for faults and stratigraphic features: The Leading Edge, **14**, 1053–1058, <https://doi.org/10.1190/1.1437077>.
- Bakker, P., 2003, Image structure analysis for seismic interpretation: Ph.D. thesis, Technische Universiteit Delft.
- Bednar, J. B., 1998, Least-squares dip and coherency attributes: The Leading Edge, **17**, 775–776, <https://doi.org/10.1190/1.1438051>.
- Bulhoes, E. M., 1999, Técnica “Volume de Amplitudes” para mapeamento de feicoes estruturais: Anais do VI Congresso Internacional da Sociedade Brasileira de Geofisica (in Portuguese).
- Bulhoes, E. M., and W. de Amorin, 2005, Principio da sismocamada elementar e sua aplicacao a tecnica de volume de amplitudes (TecVa): Anais Ninth International Congress of the Brazilian Geophysical Society (in Portuguese).
- Castagna, J. P., S. Sun, and R. W. Siegfried, 2003, Instantaneous spectral analysis: Detection of low-frequency shadows associated with hydrocarbons: The Leading Edge, **22**, 120–127, <https://doi.org/10.1190/1.1559038>.
- Chopra, S., J. P. Castagna, O. Portniaguine, 2006, Seismic resolution and thin-bed reflectivity inversion: CSEG RECORDER, **31**, 1, 19–25.
- Chopra, S., and K. J. Marfurt, 2007, Seismic attributes for prospect identification and reservoir characterization: Geophysical Development Series, SEG.
- Chopra, S., J. P. Castagna and Y. Xu, 2009, Thin-bed reflectivity inversion and some applications: First Break, **27**, 27–34.
- Chopra, S., S. Misra, and K. J. Marfurt, 2011, Coherence and curvature attributes on preconditioned seismic data: The Leading Edge, **21**, 386–393, <https://doi.org/10.1190/1.3575281>.
- Chopra, S., and K. J. Marfurt, 2007, Seismic attributes for prospect identification and reservoir characterization: SEG Geophysical Development Series, 11.
- Chopra, S., and K. J. Marfurt, 2015, Choice of mother wavelets in CWT spectral decomposition: 83rd Annual International Meeting, SEG, Expanded Abstracts, 2957-2961.
- Chopra, S., and K. J. Marfurt, 2016, Spectral decomposition and spectral balancing of seismic data, The Leading Edge, **26**, 936–939.
- Fahmy, W. A., G. Matteucci, J. Parks, M. Matheney, and J. Zhang, 2008, Extending the limits of technology to explore below the DHI floor; successful application of spectral decomposition to delineate DHIs previously unseen on seismic data: 78 Annual International Meeting of the SEG, Expanded Abstracts, 408–412.
- Honorio, B. C. Z., M. C. de Matos, and A. C. Vidal, 2017, Similarity attributes from differential resolution components: Interpretation, **5**, T65–T73, <https://doi.org/10.1190/INT-2015-0211.1>.
- Gersztenkorn, A. and K. J. Marfurt, 1999, Eigenstructure-based coherence computations as an aid to 3D structural and stratigraphic mapping: Geophysics, **64**, 1468–1479, <https://doi.org/10.1190/1.1444651>.
- Goupillaud, P., A. Grossman, and J. Morlet, 1984, Cycle-octave and related transforms in seismic signal analysis: Geoexploration, **23**, 85–102, [https://doi.org/10.1016/0016-7142\(84\)90025-5](https://doi.org/10.1016/0016-7142(84)90025-5).
- Li, F. Y., and W. K. Lu, 2014, Coherence attribute at different spectral scales: Interpretation, **2**, SA99–SA10, <https://doi.org/10.1190/INT-2013-0089.1>.

- Mallat, S., and Z. Zhang, 1993, Matching pursuits with time-frequency dictionaries: *IEEE Transactions on Signal Processing*, **41**, 3397–3415, <https://doi.org/10.1190/1.1444415>.
- Marfurt, K. J., R. L. Kirlin, S. H. Farmer, and M. S. Bahorich, 1998, 3-D seismic attributes using a running window semblance-based algorithm: *Geophysics*, **63**, 1150–1165, <https://doi.org/10.1190/1.1444415>.
- Marfurt, K. J., 2017, Multispectral coherence: 79th Annual EAGE Conference and Exposition, Expanded Abstract, (to be presented).
- Marfurt, K. J. and R. L. Kirlin, 2001, Narrow-band spectral analysis and thin-bed tuning, *Geophysics*, **66**, 1274–1283, <https://doi.org/10.1190/1.1487075>.
- Marfurt, K. J., 2006, Robust estimates of reflector dip and azimuth: *Geophysics*, **71**, P29–P40, <https://doi.org/10.1190/1.2213049>.
- Partyka, G. A., J. Gridley, and J. Lopez, 1999, Interpretational applications of spectral decomposition in reservoir characterization: *The Leading Edge*, **18**, 353–360, <https://doi.org/10.1190/1.1438295>.
- Pepper, R., and G. Bejarano, 2005, Advances in seismic fault interpretation automation, AAPG Search and Discovery Article 40170, <http://www.searchanddiscovery.com/documents/2005/pepper/>.
- Sinha, S., P. S. Routh, P. D. Anno, and J. P. Castagna, 2005, Spectral decomposition of seismic data with continuous-wavelet transform: *Geophysics*, **70**, P19–P25, <https://doi.org/10.1190/1.2127113>.
- Stockwell, R.G, L. Mansinha, R. P. Lowe, 1996, Localization of the complex spectrum: the S transform, *IEEE Transactions on Signal Processing*, **44**, 998–1001.
- Sui, J.-K., X.-D. Zheng, and Y.-D. Li, 2015, A seismic coherency method using spectral attributes: *Applied Geophysics*, **12**, 353–361.
- Vernengo, L., and E. Trincherro, 2015, Application of amplitude volume technique attributes, their variations, and impact: *The Leading Edge*, **25**, 1246–1253, <https://doi.org/10.1190/tle34101246.1>.